Comparative Analysis of Brightness-Based Laser-Induced Fluorescence (BBLIF) and Structured Planar Laser-Induced Fluorescence (S- PLIF) for Film Thickness Measurement in Two-Phase Flow

Sherif A. A, Johnson, K., Hann D. B.*

The University of Nottingham, UK
*Corresponding author: david.hann@nottingham.ac.uk

Keywords: Brightness based LIF, Multiphase fluids, Structured planar LIF,film thickness.

ABSTRACT

Improved understanding of the interactions between gas and liquid phases in gas sheared film flow is crucial for improved capability to employ computational modeling in the future to optimise systems, thereby reducing environmental impact, increasing efficiency, and enhancing productivity. This abstract compares two techniques for measuring the thickness of the film in different regimes visible in a rectangular cross-section gas-sheared liquid film rig, namely previously published Brightness Based Laser Induced Fluorescence (BBLIF) data and Structured Planar Laser Induced Fluorescence (S-PLIF) from the current investigation. The study presents and compares examples at a specific liquid flow rate (8 litres per minute) for superficial gas velocities in the range 1 ms^{-1} to 10 ms^{-1}, noted as being in different flow regimes. The investigation reveals that the S-PLIF technique produces results that are within the uncertainty bands of the BBLIF data for most scenarios. However, in the transition regime, statistical variations emerge. The frequency content of the two film heights is analyzed using a Hilbert-Huang Technique. This shows clearer results for the S-PLIF than for BBLIF which is attributed to the erratic values that can occur in BBLIF when total internal reflection occurs. It is concluded that the S-PLIF technique demonstrates promise as a reliable method for determining film thickness which is highly advantageous as it can be applied to images obtained with seeded flow intended for PIV analysis. The S-PLIF film thickness data can be used for generating automated masks for PIV analysis concurrently conducted in both the gas and liquid phases. This advancement facilitates enhanced capability to advance understanding of complex fluid dynamics and optimise system performance.

1. Introduction

The understanding of the interactions between the gas and liquid phases in two-phase flow is pivotal to numerous industrial and scientific processes. The film thickness in two-phase flows is a key determinant of heat transfer efficiency, mass transfer rates, and overall system performance in applications, ranging from heat exchangers to aircraft bearing chambers. Specifically, for stratified

or annular gas/liquid flow in a pipe, the pressure drop along a pipe is related to the thickness of the film, along with the roughness of that film. Consequently, the ability to be able to measure the film thickness accurately and precisely at a point, along a line, or over an area holds great significance for a wide range of industrial and scientific applications.

Over the last decade, several optical techniques have emerged to identify the spatial and temporal variation in film thickness. These methods offer excellent alternatives to intrusive measurement techniques, as they do not impact fluid properties or flow characteristics during measurement. Noteworthy techniques include direct imaging [Sinha et al. (2022)], **PLIF** (Planar Laser Induced Fluorescence) [Dulin et al. (2023); Zadrazil et al. (2014)] and **BBLIF** (Brightness Based Laser Induced Fluorescence) [Alekseenko et al. (2014); A. V. Cherdantsev (2023); A. Cherdantsev et al. (2023)]. While direct imaging, when properly calibrated, provides information on film thickness it is limited to specific situations requiring two directions of access to the film surface for reliable results [Sinha et al. (2022)]. Previously it has been used to identify the interface of the liquid phase for automated masking when comparing the velocity field of two phases [Kim et al. (2022)]. However, it was discovered that this put a limitation on the maximum gas velocity that could be studied. When the film was in the 3D regime, with transition occurring at a gas speed of about 5 m/s for water-air flows, the 3D nature of the waves made it harder to identify the surface [Kim et al. (2022)].

Until 2019, PLIF was considered a reliable technique offering high-resolution data on the film thickness in two-phase flow. It has also been combined with PIV to produce detailed velocity information in downward annular flow [Zadrazil et al. (2014)]. It has the advantage over direct imaging in that the fluorescent dye makes image segmentation of liquid and gas much more obvious in the images. However, access from two directions is essential in order to get measurements. BBLIF has the advantage of yielding the measurement of film thickness over a surface, with high spatial and temporal resolution [A. V. Cherdantsev (2023)]. In addition, it is feasible to measure a 2D surface with optical access from only one direction which has many advantages in complex geometry situations. The main complications are in calibrating the images for the conversion of intensity to film height particularly when looking at 2D areas [A. V. Cherdantsev (2023); A. V. Cherdantsev et al. (2014)].

A somewhat unexpected finding by Cherdantsev et al. [A. V. Cherdantsev et al. (2019)] was that PLIF was not always identifying the true film thickness, but instead was identifying the thickness based on reflections of the surface rather than the interface itself. In contrast, BBLIF offered a better correlation with the true thickness of the film (established via direct image scrutiny) in most cases, except for instances when the waves were steep when BBLIF overpredicts the film thickness significantly. Further investigation of the discrepancy led to the development of a new technique called S-PLIF (Structured Planar Laser Induced Fluorescence) [Charogiannis et al. (2019)]. Like PLIF, S-PLIF employs a structured light sheet, deliberately forming streaks that change direction at

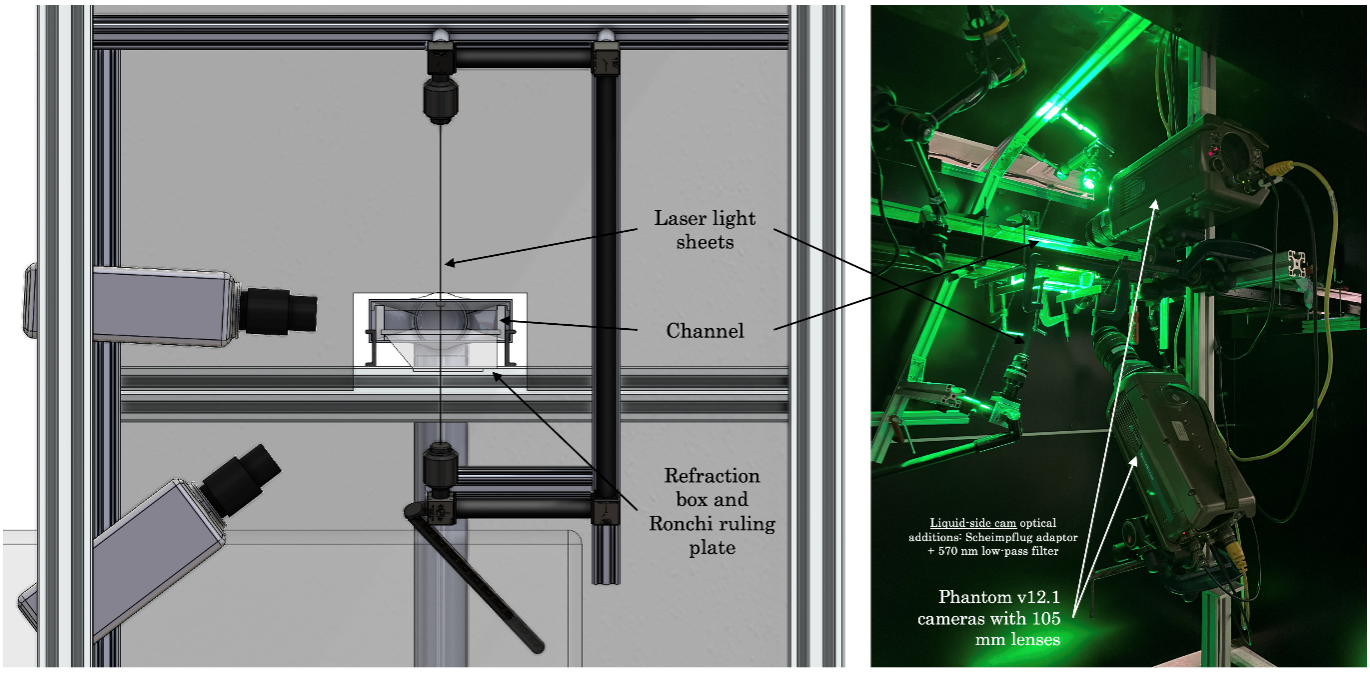

Figure 1. (left) CAD image of the apparatus used to measure the 2 phases and identify the interface. (right)Photograph of the apparatus.

the interface making it easier to detect accurately. This paper compares the S-PLIF results obtained using the University of Nottingham gas-sheared liquid flow rig, as described in Section 2, to those obtained using BBLIF at a different time in the same rig.

2. Summary of the two methodologies

The experiments were conducted in a rectangular cross-section gas-sheared liquid flow rig featuring at the University of Nottingham (illustrated in Figure 1.). A more detailed description of this rig can be obtained from previous publications [A. V. Cherdantsev et al. (2014); A. V. Cherdantsev (2023); Hann et al. (2018)].

BBLIF results were taken in a prior study, at superficial gas velocities (V_{gs}) between 1 ms^{-1} and 24 ms^{-1} and for liquid flow rates Q_f between 1 lpm (litres per minute) and 8 lpm. These BBLIF results are documented in [A. V. Cherdantsev (2023)].

S-PLIF results, acquired during the current study, with similar gas and liquid flow rates, are the focus of this paper. Specifically, this paper focuses on a subset of this data, representing measurements within distinct flow regimes identified in the gas-sheared rig - the 2D regime, the transition regime, the 3D regime, and the roll wave regime. Further details regarding regime transition boundaries can be found in Cherdantsev [A. V. Cherdantsev (2023)].

S-PLIF was employed to precisely identify the interface serving as a more accurate alternative to direct imaging such as used in [Kim et al. (2022)]. This identified interface was used to act as a mask for conducting PIV analysis of images obtained simultaneously in both the liquid and the gas phases and that work is communicated a parallel paper submitted to this conference Sherif et al. (2025). Refer to Figure 1a) for a CAD image of the optical set-up of the apparatus used to produce the two-phase measurements and Figure 1b)for a photograph showing the rig in operation. The lower camera captures images through a refraction box of a specific shape allowing the utilisation of Schlieren optics to image the liquid from below the duct.

3. Example of the results

In comparing the two techniques (S-PLIF and BBLIF) in this paper, a choice was made to focus on measurements taken at the 8 lpm liquid flow rate, specifically focusing on instances corresponding to the 2D wave, transition region, 3D wave, and Roll wave regimes. Statistics from the BBLIF results taken previously have already been detailed in another publication [A. V. Cherdantsev (2023)].

Figure 2 displays two S-PLIF images from the rig illustrating the specific issue of the false interface. In the upper image, it is evident that the structured light changes direction before reaching what was initially perceived as the true interface. This suggests that the top surface is a false representation generated by the reflection of structured light, and the actual surface is where the structured light changes direction. This discrepancy becomes even more pronounced in the lower image of Figure 2, where the pebbled surface resulting from the 3D flow gives rise to bright areas that are noticeably distant from the actual surface.

An in-house cross-correlation algorithm has been developed to identify the change in direction of the structured light compared to reference images of the structured light in a flooded duct (ie with the duct filled with water). The algorithm comparing the flooded duct images to the sheared flow images gives us the true surface. In the full application of this work, this surface definition is used to automatically produce image-specific masks, that are applied to images from both cameras enabling phase-specific PIV analysis Sherif et al. (2025). However, it was noted that the interface information can also be analysed to give vital information about film dynamics. This is the focus of this paper.

A useful tool for understanding the surface wave parameters is a space-time diagram where a slice of the flow along the duct is plotted with time as shown in Figure 3. The two figures shown are for a superficial gas velocity of 6 ms^{-1} and demonstrate that the S-PLIF derived data (left-hand image) and the BBLIF derived data (right-hand image) have similar characteristics. The similar gradients demonstrate that the detected waves are moving at the same speed and have similar frequencies. The BBLIF image includes annotated and visible bright spots which are a well-known

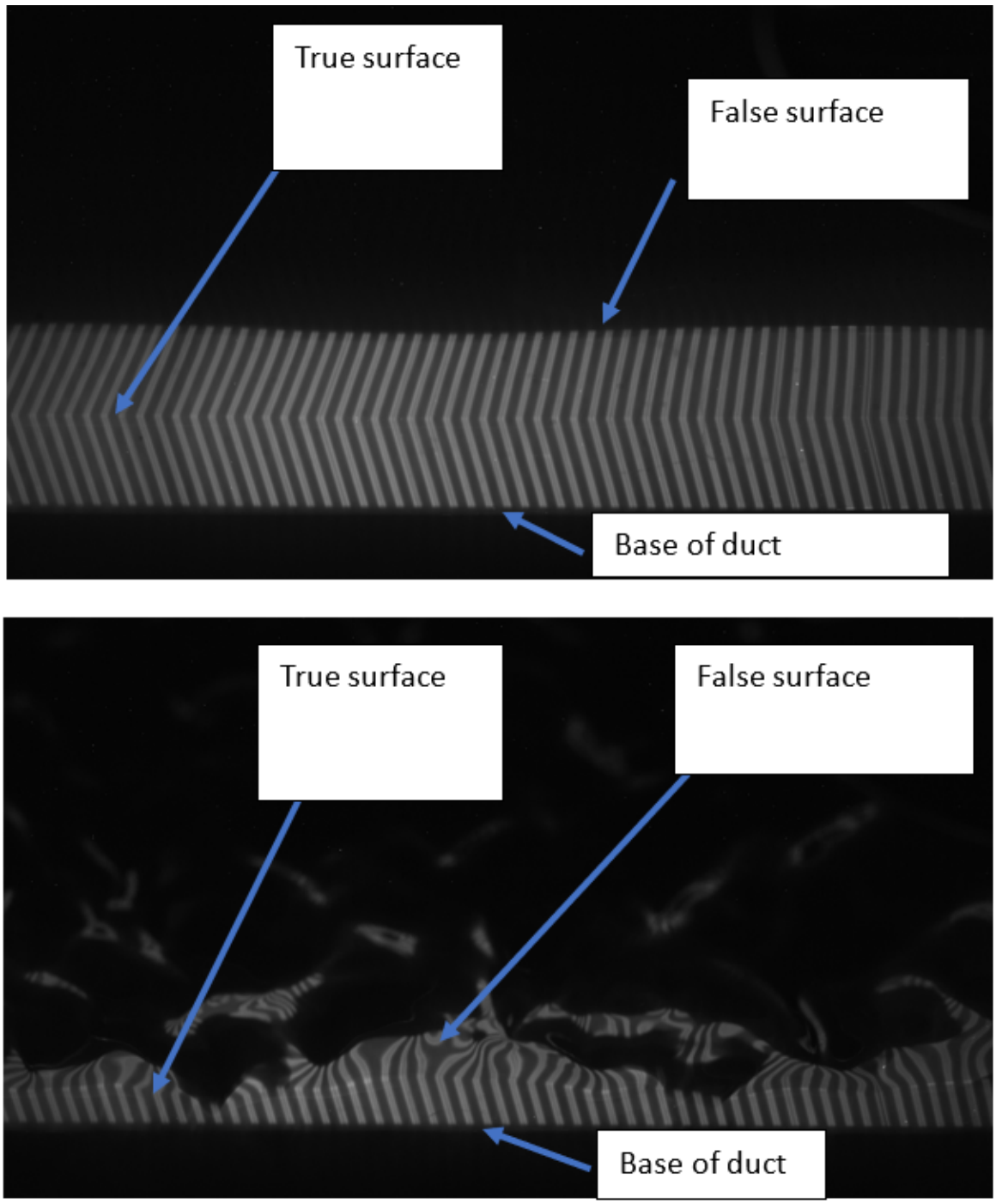

Figure 2. (upper) SPLIF results at 1 m/s. (lower) SPLIF results at 6 m/s. Identified in the image are the base of the duct, the true surface, and the false surface which has previously been falsely identified as the thickness of the film.

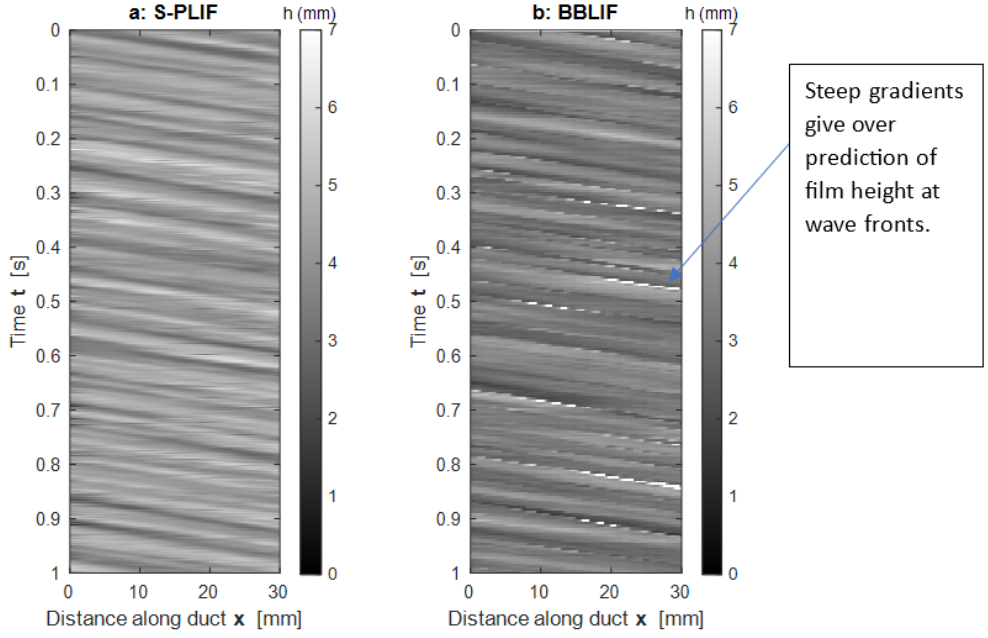

Figure 3. Space-time diagrams showing how the interface changes along the duct with time. V_{gs}=6 m/s. Q_f=8lpm. (a) results from the S-PLIF algorithm. (b) results from the BBLIF algorithm taken separately.

issue with steep gradients causing total internal reflections. BBLIF has a lower spatial resolution which explains the obvious pixelation in the right image.

Figure 4 shows the Probability density functions (PDF) of the film height extracted from the S-PLIF images. The data is for a liquid flowrate of 8lpm and superficial gas velocities between 1 ms^{-1} and 10 ms^{-1}. The PDFs are obtained by extracting film height from the centre column of each image and applying statistical analysis. The PDF of the wave heights is narrower and only slightly negatively skewed at low gas velocity, reflecting that the troughs are somewhat less deep than the waves above the median film thickness. The PDFs broaden and become more negatively skewed as the superficial gas velocity increases indicating more variation in film height as would be expected in the 3D wave flow regime. For this liquid flow rate transition from 2D to 3D waves occurs at a superficial gas velocity of around 3-4 ms^{-1}. Above 6 m/s the PDF becomes positively skewed since the most probable thickness is the base film thickness and it only occasionally has a wave passing by.

The data from the PDF's of the S-PLIF can be compared to the statistics of the BBLIF as shown in Figure 5. The grey-scale background image in the figure represents the PDF data for the S-PLIF results with the colourscale bar on the right showing the grey shades that correspond to each PDF level. At each S-PLIF data point (red symbols) the median film thickness is highlighted by the graph symbol and the 0.025 and 0.975 quantiles are utlisied to establish the minimum and maximum of the film thickness data for comparison with BBLIF. The same analysis is applied to the

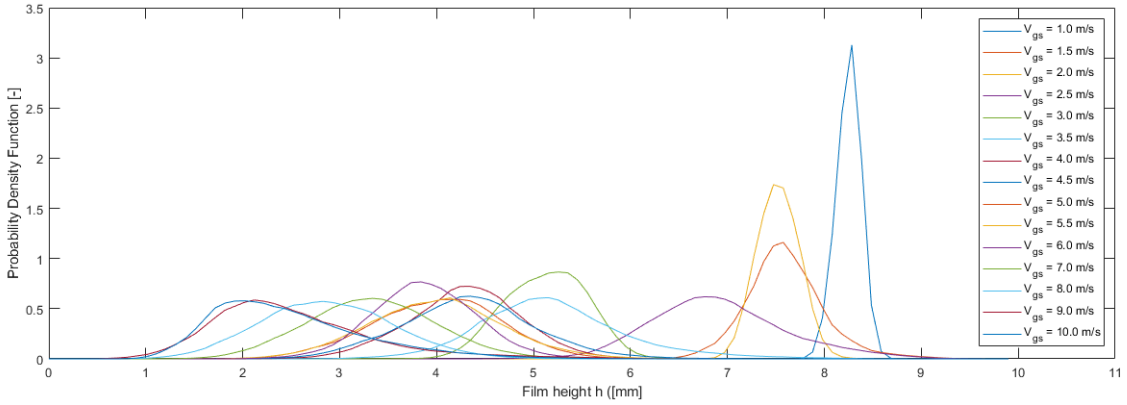

Figure 4. An S-PLIF example of the development of the probability density function for Q_f =8 lpm at various superficial gas velocities

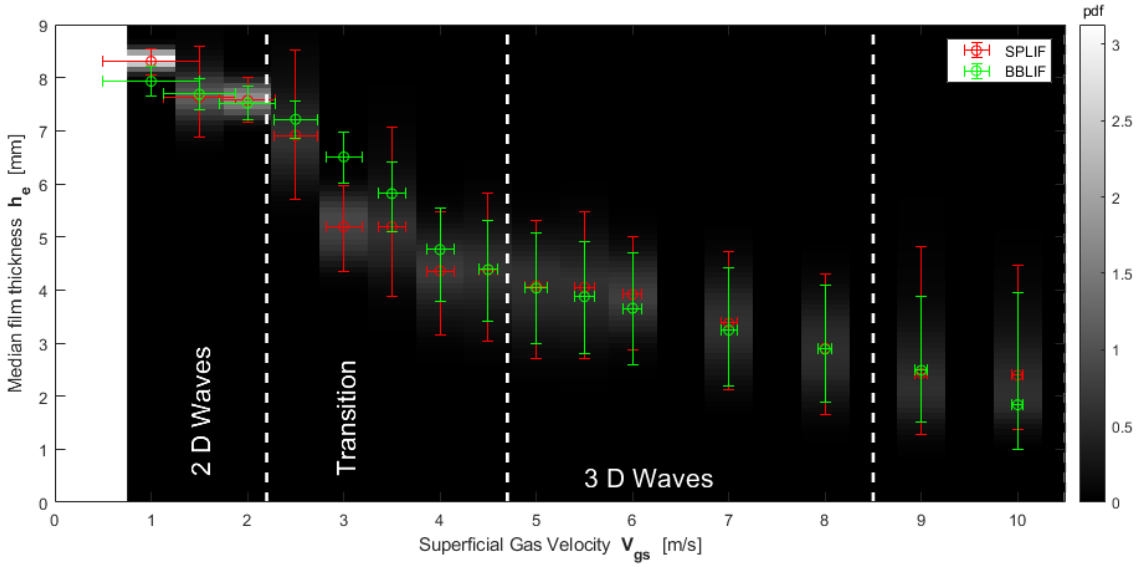

Figure 5. Comparison of statistics from S-PLIF and BBLIF. Error bars are 0.025 and 0.975 quantiles of distributions. Colours are the probability density function of the SPLIF results. Results are from Q_f = 8 lpm.

BBLIF data (green symbols). Notably, except for the transition region, the median and quantiles from both techniques are closely aligned. In the transition region, the BBLIF data yields a slightly higher film thickness value compared to the S-PLIF. The reason for this is not immediately obvious but could be due to signal length. The flow has been seen to oscillate between 3D and 2D regimes over time. It could be that the capture time preferentially favoured one regime in one set of measurements but favoured a different regime in the other.

However, other than these two points, the close correlation between the two measurement techniques suggests that the S-PLIF is a viable technique for obtaining the film thickness, and results compare better with the BBLIF than classic PLIF. The major advantage in this context of being able to use the S-PLIF values is that it has been applied to fluids with seeding particles present. This enables film thickness data to be obtained simultaneously with the PIV images so that it can be used for a mask to then obtain the velocity fields in both phases. Details of this advancement will be expanded upon in a parallel paper for this conference Sherif et al. (2025). It would not be possible to obtain simultaneous PIV images and BBLIF film thickness data because the seeding particles preclude the use of the BBLIF technique

4. Determination of the main frequencies for SPLIF and BBLIF

An advantage of having such rich data sets is that it is possible to investigate the frequency content of the signals from both BBLIF and S-PLIF data. In many publications, Fourier transforms are used to calculate the frequency of the waves. However, it is well known that Fourier analysis only works perfectly on pure sine waves. If the frequency or amplitude of the waves varies in the signal, then this variation can introduce harmonics which can combine to disguise the true frequency peak. There are various methods to overcome this, and one is the use of the Hilbert Huang transform (HHT) Huang et al. (1998). In this methodology, intrinsic mode functions are identified from the shape of the signal using a Variational Mode Decomposition technique. The instantaneous frequency and amplitude of each of these modes can be determined using the Hilbert analysis and these can be combined to produce an HHT which can be temporally average to get the marginal Hilbert Huang transform. This marginal Hilbert Huang transform has been demonstrated to be able to identify physical frequencies more accurately than Fourier analysis in non-stationary cases [Huang et al. (1998)].

Figure 6 shows an example of the surface variation and the HHT for one of the S-PLIF datasets. The analysis shows that the waves are not sinusoidal and therefore exhibit amplitude and frequency modulations as they pass this particular point. Figure 7 shows a similar example of the surface variation and the HHT for the corresponding BBLIF dataset. This is not as clear as Figure 6, because of the optical distortions and reflections that affect the values for BBLIF. There are unrealistic peaks in the BBLIF data which introduce higher order frequency and large amplitude values to the HHT.

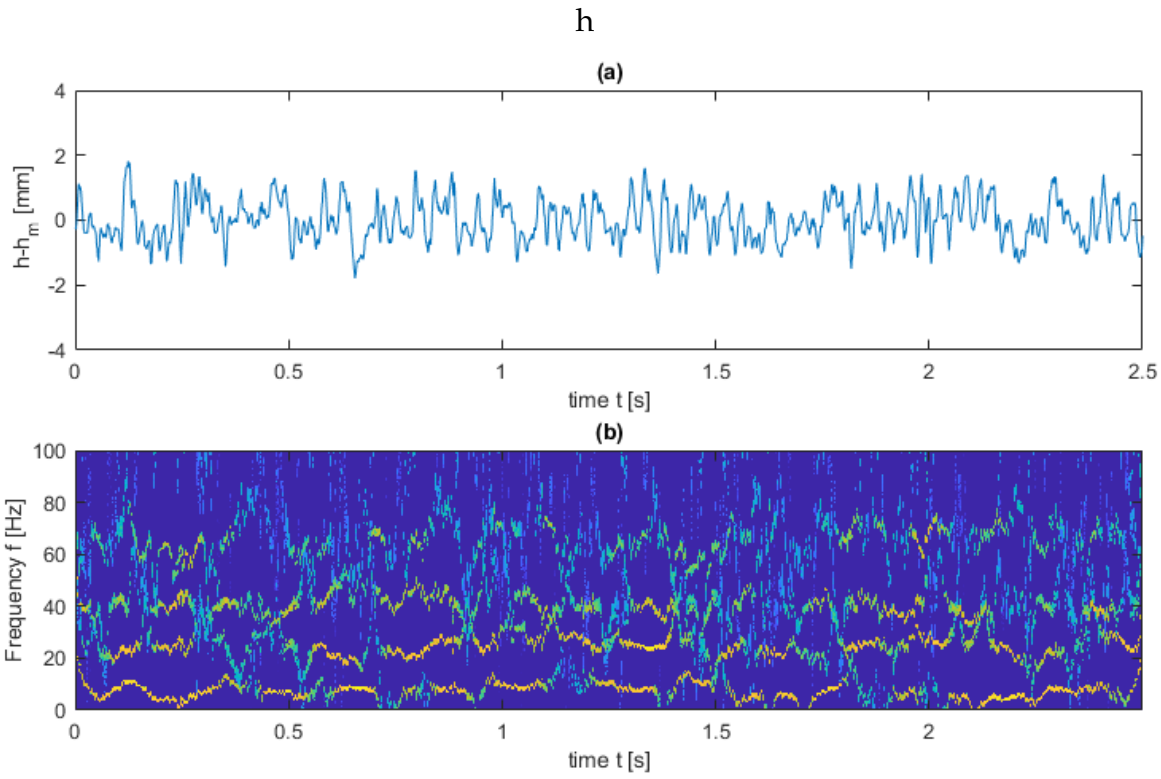

Figure 6. Example of (a) surface variation and (b) Hilbert Huang Transform of surface variation for $V_{gs} = 8ms^{-1}$ and Q_f = 8 lpm for SPLIF data.

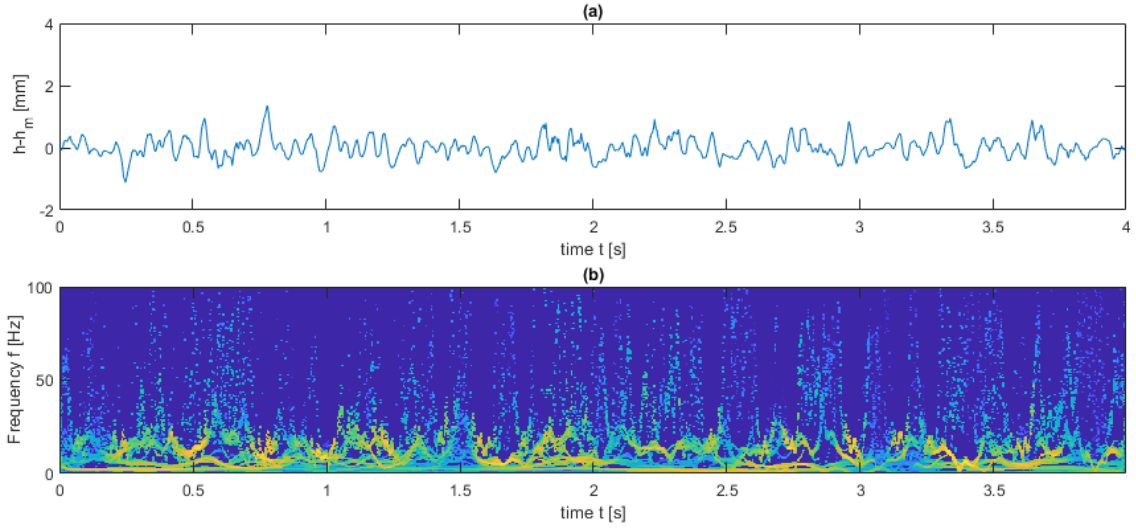

Figure 7. Example of (a) surface variation and (b) Hilbert Huang Transform of surface variation for $V_{gs} = 8ms^{-1}$ and Q_f = 8 lpm for BBLIF data.

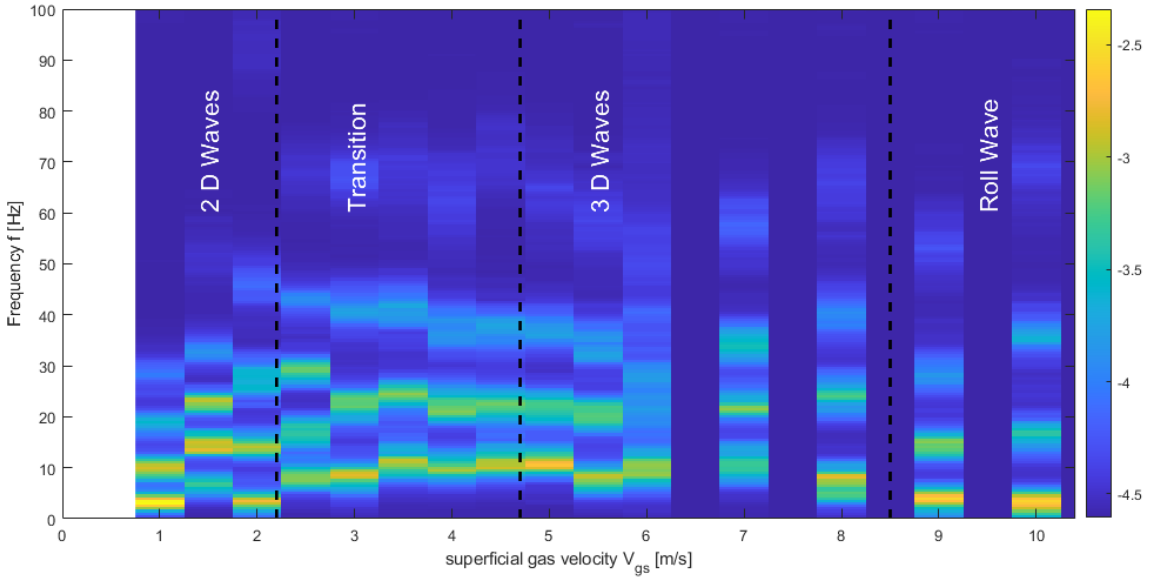

Figure 8. Marginal Hilbert Huang Transform of the SPLIF data at varying superficial gas velocities. Note the clear frequency peaks detected.

To obtain the marginal Hilbert Huang transform, the HHT is averaged with time. This is shown in Figure 8 for the SPLIF data and in Figure 9 for the BBLIF data. Figure 8 demonstrates that the fundamental frequencies present in the film height data rise and then remain stable until the 3D wave regime. after which they decrease as the superficial gas velocity increases. As we transition from the 3D to the Roll wave regime, the fundamental frequencies decrease.

Figure 9 does not show as rich a variety of frequencies. This is mainly because there are significant occasional peaks that have large amplitude due to reflections of light in BBLIF. These combine to increase low-frequency noise which is a feature of the HHT of the BBLIf.

In Figure 8 there are multiple frequencies, and in HHT analysis, these can often be linked directly to physical mechanisms. It is unclear exactly what these physical mechanisms are in this particular case, but it is reasonable to expect high-frequency ripple waves which would change speed with the thickness of the film and also the generation of roll waves at lower frequencies. It is also possible that some of the 3D waves are being reflected off the sides of the duct.

The two low frequencies in Figure 8 are linked to the positive skewness that was observed at 9 and 10 ms^{-1} which could mean that the boundary between 3D and roll waves might start around 8 ms^{-1} contrary to what was shown in [A. V. Cherdantsev (2023)].

Overall the work presented in this paper shows that the S-PLIF technique can be used to generate film thickness data comparable to that generated by BBLIF but with the advantage that it can be

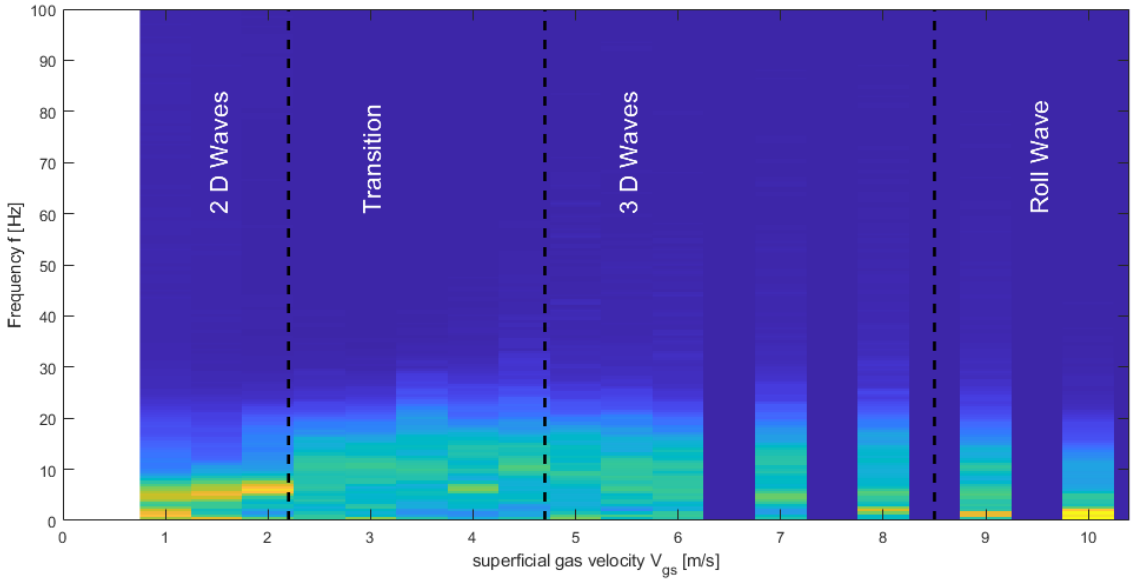

Figure 9. Marginal Hilbert Huang Transform of the BBLIF data at varying superficial gas velocities. Note the higher order frequencies created due to the unrealistic peaks of the BBLIF data.

obtained from the same images used for PIV analysis. Both S-PLIF and BBLIF data can be analysed for frequency content but there appears to be higher frequency content present in the S-PLIF data compared to the BBLIF data. This can potentially provide information about surface effects such as lower amplitude, and higher frequency ripple waves.

5. Conclusions

The main conclusions of the work presented in this paper are that

- Structured light PLIF (S-PLIF)can be used to identify the interface in two-phase gas-sheared liquid flow. This can be used to look at film height dynamics as the flow transitions from 2D to 3D to Disturbance/Roll wave regimes as the superficial gas velocity increases.
- The results of the S-PLIF and BBLIF techniques applied to data obtained from the same apparatus at different times have been compared and the results presented demonstrate that, apart from in the transition region the statistics obtained using both techniques are similar enough to conclude that S-PLIF can give a good indication of the film thickness.
- The S-PLIF technique can be combined with PIV to obtain not just the location of the interface, but also the velocity field by using the S-PLIF to generate frame-by-frame masks for the PIV analysis.

Acknowledgements

The authors would like to thank Rolls-Royce plc and the EPSRC for the support under the Prosperity Partnership Grant Cornerstone Mechanical Engineering Science to Enable Aero Propulsion Futures, Grant Ref: EP/R004951/1. The authors would also like to thank Ivan Zadrazil from Dantec Dynamics for his support and advice in developing the S-PLIF processing.

References

Alekseenko, S. V., Cherdantsev, A. V., Heinz, O. M., Kharlamov, S. M., & Markovich, D. M. (2014). Analysis of spatial and temporal evolution of disturbance waves and ripples in annular gas-liquid flow. *International Journal of Multiphase Flow*, *67*(S), 122-134.

Charogiannis, A., Sik An, J., Voulgaropoulos, V., & Markides, C. N. (2019). Structured planar laser-induced fluorescence (s-plif) for the accurate identification of interfaces in multiphase flows. *International Journal of Multiphase Flow*, *118*, 193-204.

Cherdantsev, A., Bobylev, A., Guzanov, V., Kvon, A., & Kharlamov, S. (2023). Measuring liquid film thickness based on the brightness level of the fluorescence: Methodical overview. *International Journal of Multiphase Flow*, *168*.

Cherdantsev, A. V. (2023). Three-dimensional evolution and interaction of disturbance waves on a gas-sheared liquid film on a horizontal plane near the transition region. *International Journal of Multiphase Flow*, *164*.

Cherdantsev, A. V., An, J. S., Charogiannis, A., & Markides, C. N. (2019). Simultaneous application of two laser-induced fluorescence approaches for film thickness measurements in annular gas-liquid flows. *International Journal of Multiphase Flow*, *119*, 237-258.

Cherdantsev, A. V., Hann, D. B., & Azzopardi, B. J. (2014). Study of gas-sheared liquid film in horizontal rectangular duct using high-speed lif technique: Three-dimensional wavy structure and its relation to liquid entrainment. *International Journal of Multiphase Flow*, *67*, 52-64.

Dulin, V., Cherdantsev, A., Volkov, R., & Markovich, D. (2023). Application of planar laser-induced fluorescence for interfacial transfer phenomena. *Energies*, *16*(4).

Hann, D. B., Cherdantsev, A. V., & Azzopardi, B. J. (2018). Study of bubbles entrapped into a gas-sheared liquid film. *International Journal of Multiphase Flow*, *108*, 181-201.

Huang, N. E., Shen, Z., Long, S. R., Wu, M. C., Shih, H. H., Zheng, Q., ... Liu, H. H. (1998). The empirical mode decomposition and the hilbert spectrum for nonlinear and non-stationary

time series analysis. *Proceedings of the Royal Society of London. Series A: Mathematical, Physical and Engineering Sciences*, *454*(1971), 903-995.

Kim, J. H., Hann, D. B., & Eastwick, A., C. E. Cherdantsev. (2022). Can simultaneous piv in the gas and liquid phases provide insight into the transfer of momentum between the two phases? In *20th international symposium on the application of laser and imaging techniques to fluid mechanics.*

Sherif, A. A., Hann, D. B., & Johnson, K. (2025). Characterising horizontal two-phase flows using structured-planar laser-induced fluorescence (s-plif) coupled with simultaneous two-phase piv (s2p-piv). In *not yet published, proceedings of icmf 2025.*

Sinha, A., Hann, D., Johnson, K., & Walsh, M. (2022). Experimental investigation into oil film thickness and behaviour near an aero-engine bearing. In *Proceedings of the asme turbo expo* (Vol. 8-A).

Zadrazil, I., Matar, O. K., & Markides, C. N. (2014). An experimental characterization of downwards gas-liquid annular flow by laser-induced fluorescence: Flow regimes and film statistics. *International Journal of Multiphase Flow*, *60*, 87-102.